J Solid State Electrochem (2009) 13:1553–1559
DOI 10.1007/s10008-008-0724-y

ORIGINAL PAPER

Silver electrodeposition from water–acetonitrile mixed solvents in the presence of tetrabutylammonium perchlorate

Part II—A SERS study of acetonitrile reactivity and tetrabutylammonium adsorption

Claudio Mele · Benedetto Bozzini

Received: 1 August 2008 / Revised: 3 October 2008 / Accepted: 27 October 2008 / Published online: 14 November 2008

Abstract In this paper, surface-enhanced Raman spectroscopy has been used to investigate the electrode/electrolyte interface during Ag electrodeposition from water–acetonitrile mixed solvents. The reactivity of acetonitrile during Ag electrodeposition has been monitored, promoted by the electrocatalytic activity of silver clusters electrodeposited onto the electrode surface. The effect of the addition of tetrabutylammonium cations to the mixed solvents has been investigated and its adsorption and tilting on the silver surface has been followed as a function of the cathodic overpotential.

Keywords Mixed solvents · Silver · Acetonitrile · Tetrabutylammonium perchlorate

Introduction

Recently, the use of non-aqueous or mixed solvents gained a growing interest because they offer an alternative route for several electrochemical processes, allowing limited influence of water-related electrochemical reactions as well as the possibility of solubilizing many organics [1, 2]. The study of the interfacial electrochemistry of Ag/H_2O/acetonitrile (CH_3CN) systems has received some attention in the literature [3–5]. However, limited research effort has gone so far in the electrodeposition from non-aqueous phases [6–8]. In [9], a selection of non-aqueous solvent-based plating systems has been reviewed. From the electrocatalytic literature, it results that acetonitrile with quaternary ammonium salts as supporting electrolytes exhibit electrochemical properties that render them promising as electrolytes for metal electrodeposition [5, 8, 10].

Surface-enhanced Raman spectroscopy (SERS) has been widely used to investigate the electrode/electrolyte interface in situ since the first discovery of this phenomenon in an electrochemical experiment [11]. Limited research has been made on electrodeposition from mixed solvents or in general on the electrode/electrolyte interface in non-aqueous systems; some SERS studies of silver [4] and platinum [3] in acetonitrile solution have been reported.

Acetonitrile is a very stable compound under normal ambient conditions, but under particular conditions or in the presence of powerful catalysts, it can take part in chemical reactions, typically nitriles hydrolyze to amides [12]. The hydrolysis of CH_3CN has been monitored with Raman spectroscopy in near-critical water without added catalyst [13] or in the presence of a selection of catalysts: $NbCl_2$ [14], a bisilver cryptate complex [15], different proton donors [16], $[Os(CO)_3Cl_2]_2$ [17]. In [18], quantum chemical simulation methods have been used to study the ion solvation in water–acetonitrile mixtures.

This paper is part of a series addressing the topic of Ag electrodeposition from water–acetonitrile mixed solvents. In a previous paper [19], we investigated the nucleation of silver by electrochemical methods (cyclic voltammetry and potentiostatic current transients) and the nucleation and growth morphology by scanning electron microscopy. In the present paper, we use SERS spectroscopy to study the electrode/electrolyte interface during Ag electrodeposition from water–acetonitrile mixed solvents. We monitor the reactivity of acetonitrile during Ag electrodeposition, at environmental temperature and pressure. Moreover, we also investigated the effect of the addition of the specifically

C. Mele (✉) · B. Bozzini
Dipartimento di Ingegneria dell'Innovazione,
Salento University (formerly Lecce University),
via Monteroni,
73100 Lecce, Italy
e-mail: claudio.mele@unile.it

adsorbing tetrabutylammonium cation to mixed solvents as a supporting electrolyte for solutions with a high organic content and as a grain refiner for Ag electrodeposits.

Experimental

The Ag electrodeposition baths employed in this research were: (1) CH_3CN, $NaClO_4$ 0.1 M, $AgNO_3$ 10 mM, to this anhydrous solution controlled amounts of water were added; (2) $NaClO_4$ 0.1 M, $AgNO_3$ 10 mM with a H_2O/CH_3CN mixture with 25 vol.% of organic; (3) aqueous solution containing $NaClO_4$ 0.1 M, $AgNO_3$ 10 mM, tetrabutylammonium perchlorate (TBAP) 0.1 M; (4) $NaClO_4$ 0.1 M, $AgNO_3$ 10 mM, TBAP 0.1 M with the H_2O/CH_3CN mixture of point (2). The solutions were prepared from analytical grade chemicals supplied by Fluka and Aldrich, 99.8% HPLC-grade acetonitrile and ultra-pure water with 18.2 MΩ cm of resistivity from a Millipore-Milli-Q system.

SERS measurements were carried out with a Raman microprobe system (LabRam Jobin-Yvon) equipped with a confocal microscope, CCD detector, and interferometric and holographic notch filters. Excitation at 632.8 nm was provided by a He–Ne laser, delivering 7 mW at the sample surface. A 50× long-working-distance objective was used. In situ spectroelectrochemistry was carried out in a Ventacon cell with a vertical polycrystalline Ag disc working electrode (WE) of diameter 7 mm embedded in a Teflon cylindrical holder. A metallographic polishing procedure, consisting of wet grinding with 2400 grit SiC paper, allowed excellent reproducibility. The counter electrode (CE) was a Pt wire loop (1.25 cm^2) concentric and coplanar with the WE disc. An Ag/AgCl (KCl 3 M) reference electrode (RE) was used, placed in a separate compartment; potentials are reported on the Ag/AgCl scale. The RE probe tip was at 3 mm from the rim of the WE disc. Raman intensities are normalized over the acquisition time and proportional to the discharge current of the CCD element corresponding to a given Raman shift, uncorrected for quantum efficiency. The acquisition time of SERS spectra was 10 s.

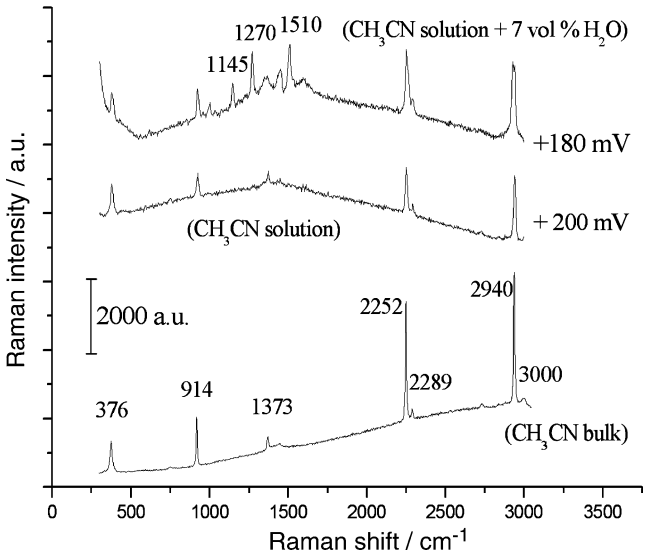

Fig. 1 In situ SERS spectrum recorded during Ag electrodeposition from anhydrous CH_3CN solution containing $NaClO_4$ 0.1 M, $AgNO_3$ 10 mM, at 200 mV, and upon addition of 7 vol.% of water, at 180 mV. A Normal Raman spectrum of acetonitrile, recorded in the bulk of the solution, is also reported for comparison

Table 1 Band assignment for Raman spectra of Fig. 1

Raman shift (cm^{-1})	Vibration (13, 22 s)
376	C—C≡N bending
914	C—C skeletal
1,373	CH_3 symmetrical deformation
2,252	C≡N stretching
2,289	C≡N stretching
2,940	CH_3 asymmetric stretching
3,000	C—H stretching

Results and discussion

A metallographically polished Ag electrode, immersed in the electrodeposition bath (1) exhibits an open-circuit potential (OCP) of 280 mV. The acquisition sequence of SERS spectra was the following: the potential was stepped in intervals of 10 mV in the cathodic direction from OCP up to 180 mV. The WE was polarized at the set potential for 1 min before acquiring the SERS spectra. No measurable changes in spectral patterns are found across the potential range investigated, the small differences in the band intensities being related to the variation of the fluorescence effect among the spectra due to the gradual silver deposition. A typical surface spectrum, measured at 200 mV, is shown in Fig. 1, together with the Normal Raman spectrum of liquid acetonitrile obtained in the same cell; the corresponding band assignment is proposed in Table 1. A perfect correspondence of the bands is found between the surface and bulk Raman spectra.

At a fixed potential of 180 mV, time-dependent SERS spectra were collected, but no significant differences were observed in the spectra measured over an interval of 10 min.

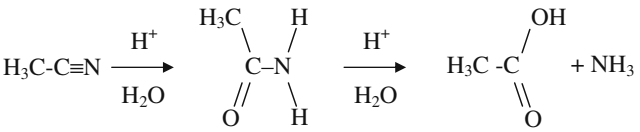

Fig. 2 Proposed mechanism for acetonitrile hydrolysis

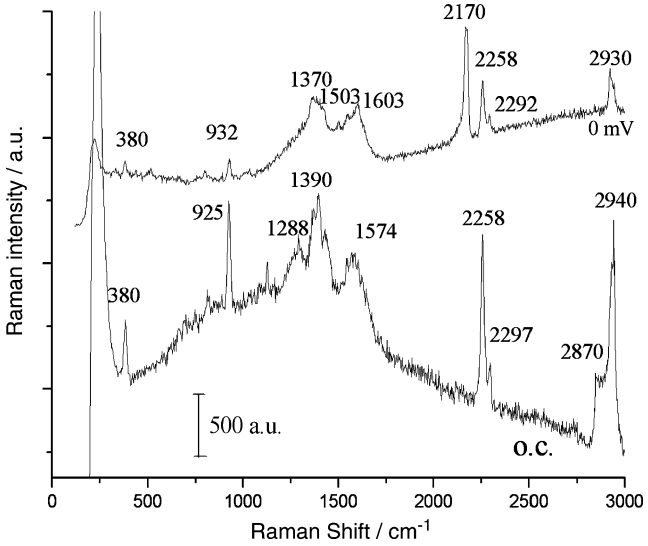

Fig. 3 In situ SERS spectra recorded at open circuit and during the Ag electrodeposition (V=0 mV) from the aqueous solution containing CH_3CN 25 vol.%, $NaClO_4$ 0.1 M, and $AgNO_3$ 10 mM

New bands appear upon addition of 7 vol.% of water to the anhydrous CH_3CN solution at (1) 1,145 cm^{-1}, (2) 1,510 cm^{-1}, and (3) 1,270 cm^{-1} (Fig. 1). These bands can be attributed to NH_2 stretching, NH_2 deformation of CH_3CONH_2, and C=O stretching of CH_3COOH, respectively. As proposed in [13–15], these features are diagnostic of CH_3CN hydrolysis in water, going on in two steps: (1) acetonitrile reacts with a molecule of water to produce acetamide; (2) acetamide reacts with a further molecule of water, to give acetic acid and NH_3. This mechanism is illustrated in Fig. 2.

The C≡N stretching of CH_3CN (2,252 cm^{-1}) in Fig. 1 does not disappear, as in [13]; this is probably due to the better time resolution and to the time-dependent nature of our experiments.

Our spectroscopic results essentially correspond to hydrolysis of CH_3CN in water described in [13–15], but in our experiments the reactivity is obtained at ambient temperature and pressure and without use of an extraneous catalyst. The reactivity we highlighted is probably due to the electrocatalytic activity of the silver clusters forming onto the electrode surface during electrodeposition.

The effect of the potential on the reactivity of acetonitrile during Ag electrodeposition has been studied in depth measuring potential-evolved SERS spectra with the solution containing $NaClO_4$ 0.1 M, $AgNO_3$ 10 mM, and CH_3CN in a volume fraction of 25%. In addition to the above-described new bands, the effect of cathodic polarization can be noticed in Fig. 3, where a spectrum collected at OCP is compared with one corresponding to a high cathodic overpotential (V=0 mV). A clearly visible peak shows up at 2,170 cm^{-1} that can be assigned to CN^- arising from the decomposition of CH_3CN. This process has been proved to occur at high cathodic overpotentials and has been observed in previous studies on Ag [3, 4, 20, 21].

The effects of the TBAP cation were also studied in the aqueous and water–acetonitrile mixed electrolytes. Potentiostatic experiments with the solution containing $NaClO_4$

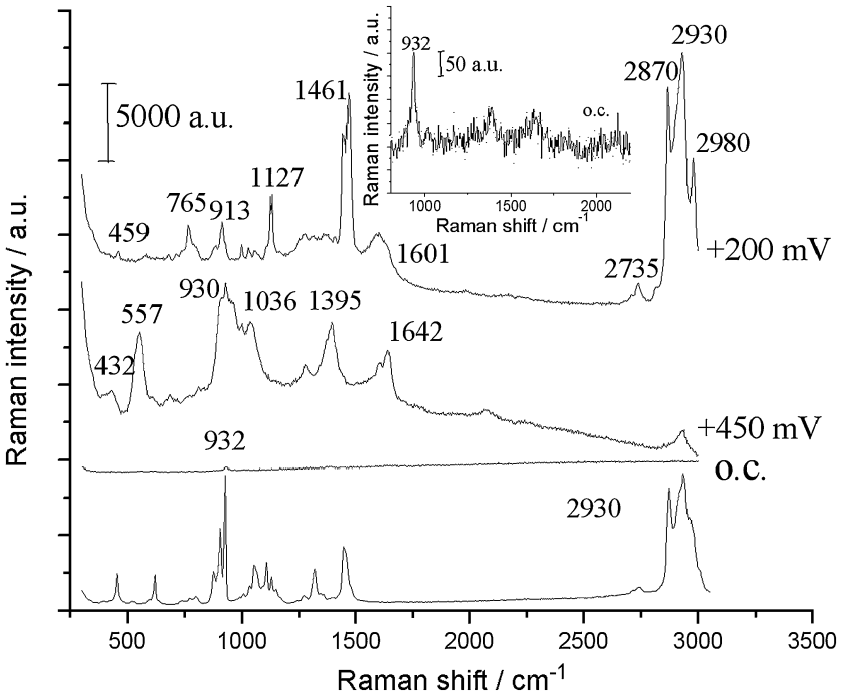

Fig. 4 In situ SERS spectra recorded at open circuit and during the Ag electrodeposition (V=200 mV) from the aqueous solution containing $NaClO_4$ 0.1 M, $AgNO_3$ 10 mM, and TBAP 0.1 M. A Normal Raman spectrum of tetrabutylammonium perchlorate is also reported for comparison

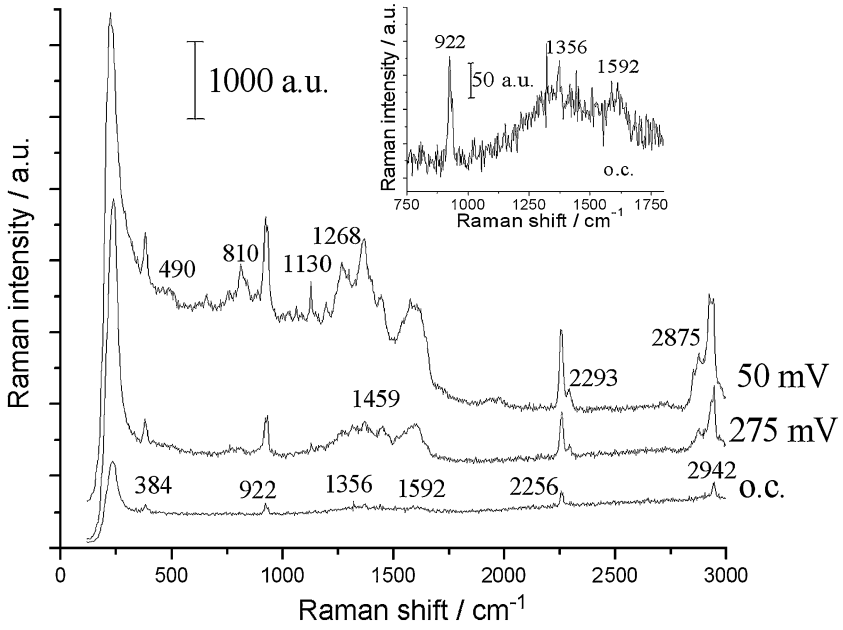

Fig. 5 In situ SERS spectra recorded at open circuit and during the Ag electrodeposition from the aqueous solution containing CH_3CN 25 vol.%, $NaClO_4$ 0.1 M, $AgNO_3$ 10 mM, and TBAP 0.1 M

0.1 M, $AgNO_3$ 10 mM, and TBAP 0.1 M were performed in the potential range from OCP (V_0=+470 mV) to +200 mV; some representative in situ SERS spectra are shown in Fig. 4. In Fig. 4, the Normal Raman spectrum of tetrabutylammonium perchlorate powder is also reported for comparison.

Spectra recorded at OCP exhibit a peak at 930 cm^{-1}, clearly visible at all potentials, corresponding to C—C skeletal vibration [13, 22]. Polarizing the WE in the cathodic range ($V = +450 \div +375$ mV), a set of new features are found, related to TBAP: a peak at 2,930 cm^{-1}, assigned to the CH_3 asymmetric stretching [22]; a peak at

Table 2 Band assignment for Raman spectra of Fig. 3, 4, and 5

H_2O 75%, CH_3CN 25% $AgNO_3$+$NaClO_4$		H_2O 100% $AgNO_3$+$NaClO_4$+TBAP			H_2O 75%, CH_3CN 25% $AgNO_3$+$NaClO_4$+TBAP			
o.c.	0 mV	o.c.	450÷375 mV	350÷200 mV	o.c.	335÷275 mV	100÷0 mV	
380	380				384	384	384	C—C≡N bending
			432	459				C—H deformation
			557				490	CH_3 rocking
				765			810	CH_2 rocking
925	932	930	930	913	922	932	932	C—C skeletal
			1,036	1,036				ClO_4^- stretching
							1,130	NH_2 stretching of CH_3CONH_2
1,288							1,268	C=O stretching of CH_3COOH
1,390	1,370		1,395		1,356	1,368	1,368	CH_3 symmetrical deformation
				1,461		1,459	1,452	CH_2 scissoring
	1,503							NH_2 deformation of CH_3CONH_2
1,574	1,603		1,642	1,601	1,592	1,592		NH_3^+ scissoring
	2,170							CN^-
2,258	2,258				2,256	2,256	2,256	C≡N stretching
2,297	2,292					2,293	2,293	C≡N stretching
				2,735				CH_2 wagging deformation
2,870				2,870		2,875	2,875	CH_3 symmetric stretching
2,940	2,930		2,930	2,930	2,942	2,942	2,942	CH_3 asymmetric stretching
				2,980				CH_3 asymmetric stretching

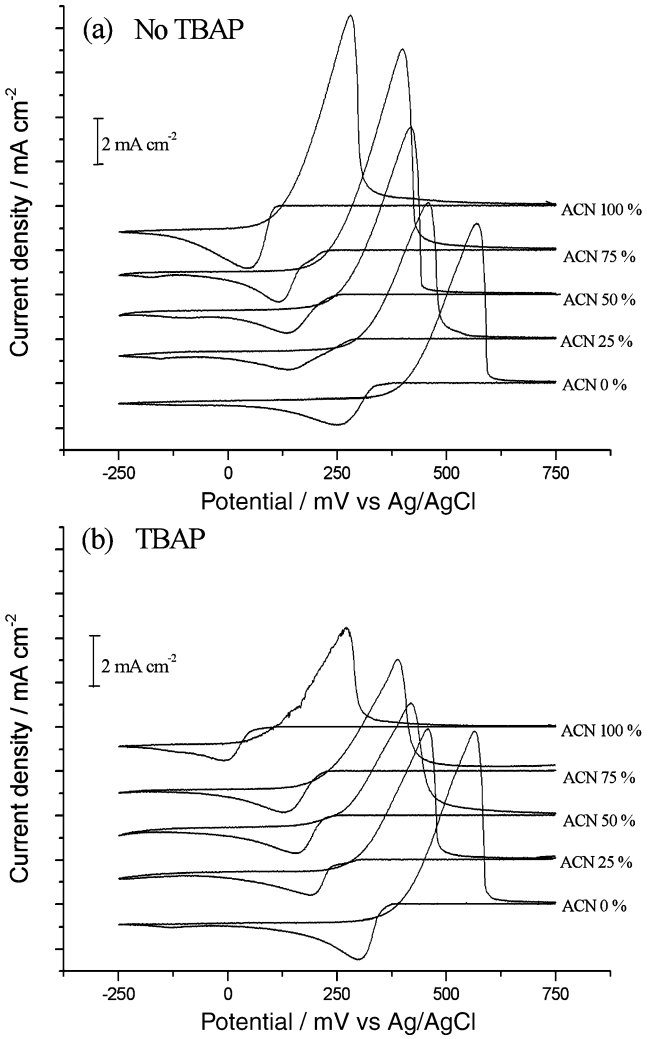

Fig. 6 Linear-sweep voltammograms for Ag electrodeposition from solutions containing $NaClO_4$ 0.1 M, $AgNO_3$ 10 mM, CH_3CN in the volume fraction indicated, **a** without TBAP and **b** with TBAP 10 mM. Working electrode: glassy carbon disk. Scan rate 10 mV s^{-1}

1,642 cm^{-1}, assigned to the scissor deformation of the NH_3^+ group; a peak at 1,395 cm^{-1}, assigned to the CH_3 symmetrical deformation [13, 22, 23]; two peaks at 432 and 557 cm^{-1}, assigned to CH deformation and CH_3 rocking [24, 25]. Moreover, a band at 1,036 cm^{-1} can be noticed, corresponding to the ClO_4^- stretching mode [24]. The presence of TBAP-related peaks witnesses adsorption of this quaternary ammonium compound on the growing Ag already from low cathodic overpotentials. The bands observed in Figs. 3, 4, and 5 are listed and interpreted in Table 2. At more cathodic potentials ($V = +350 \div +200$ mV), some changes in spectral pattern can be noticed. In particular, the features at 432, 557, and 1,395, visible at low overpotentials, tend to disappear and new bands, commented below, appear. At 459 and 765 cm^{-1}, assigned to CH deformation and rock vibration of the methylene group of $(CH_2)_3$–CH_3 [22]; at 1,461 cm^{-1}, assigned to CH_2 scissors [26]; at 2,735 cm^{-1}, assigned to CH_2 wag deformation of the methylene group near the nitrogen atom; at 2,870 and 2,980 cm^{-1}, assigned to symmetric and asymmetric methyl C—H stretching, respectively. Moreover, the peaks corresponding to the C—C skeletal vibration and to the scissor deformation of NH_3^+ are found at lower Raman shifts: 913 and 1,601 cm^{-1}, respectively. These results can be interpreted in terms of tilt of TBAP adsorbed on the Ag electrode surface, upon increasing the cathodic overpotential.

Figure 5 shows in situ SERS spectra recorded at OCP (V_0=+360 mV) and during Ag electrodeposition from the aqueous solution containing CH_3CN 25 vol.%, $NaClO_4$ 0.1 M, $AgNO_3$ 10 mM, and TBAP 0.1 M. At OCP, some typical acetonitrile bands can be recognized (at 384, 922, 1,356, 1,592, 2,256, and 2,942 cm^{-1}; see also Fig. 1 and related comments). Applying low cathodic overpotentials ($V = +335 \div +275$ mV), some TBAP bands show up (at 1,459, 2,875 cm^{-1}), as in the case of the system without CH_3CN, described above, denoting TBAP adsorption. Upon increasing the cathodic overpotential, a new set of peaks can be observed. In particular, the bands at 1,130, 1,268, and 2,293 cm^{-1} are clearly visible and can be again interpreted as a piece of evidence of the reactivity of CH_3CN. The formation of new bands at 490 and 810 cm^{-1}, possibly related to TBAP (see above and Table 2), together with a more evident symmetric methyl C—H stretching peak (at 2,875 cm^{-1}), seems to confirm a different tilt of TBAP adsorbed on the Ag electrode surface at high cathodic potentials.

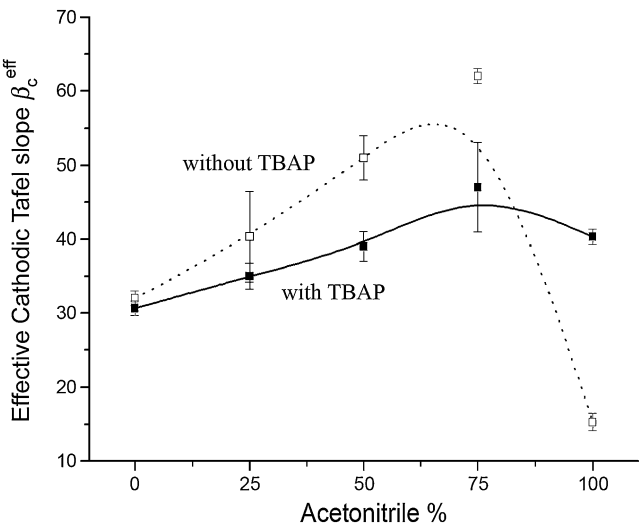

Fig. 7 Effective cathodic Tafel slope ±1 s.d., estimated from linear-sweep voltammograms obtained on glassy carbon electrode from solutions containing $NaClO_4$ 0.1 M, $AgNO_3$ 10 mM, as a function of CH_3CN percentage, without or with TBAP 10 mM. Scan rate 10 mV s^{-1}. The *lines through the data points* are just a guide to the eye

The results obtained in the present paper are consistent with the observations of the first part of our work on this topic [19], where electrokinetic effects of solvent composition have been highlighted. In order to quantify the kinetic behavior of the investigated systems, we introduced an "effective cathodic Tafel slope" β_c^{eff} that, in addition to the charge transfer information of the true Tafel slope, incorporates effect of the electrode morphology and activity. The estimate of β_c^{eff} has been performed by non-linear least squares with a model also accounting for the limiting current density i_L from the anodic going scan of our voltammetric data shown in Fig. 6. β_c^{eff} estimates are reported in Fig. 7. Higher values of β_c^{eff} can be observed with mixed electrolytes; this observation is coherent with the kinetic theory for mixed solvents presented in [1] based on ion-transfer-controlled reduction rate, predicting a maximum as a function of the organic mass fraction. Lower values of i_L can be observed with mixed electrolytes, where the reactivity of acetonitrile gives rise to the formation of Ag(I) complexes with NH_4^+ and CN^- and, correspondingly to the appearance of a new rate determining step, due to decomplexing. Moreover, with mixed solvents, the production of the Ag(I) complexes reduces the activity of Ag^+.

Spectroelectrochemical information on acetonitrile reactivity and TBAP adsorption also helps rationalize the morphological differences observed in the SEM micrographs of Ag layers deposited, varying the CH_3CN%, in the absence and in the presence of TBAP (figure 9 in [19]). In particular, the growth of crystallites tending to cluster in the cases of mixed solvents can be explained with the decreased Ag^+ activity, due to complexing with reaction products of acetonitrile, consequently reducing the critical overpotential of dendritic growth. Moreover, in these conditions, the growth is expected to be favored with respect to nucleation.

Direct observation of the adsorption of TBAP, starting from low cathodic overvoltages, is coherent with its remarkable grain-refining activity. Moreover, the presence of TBAP correlates with smaller values of the Tafel slope and limiting current density estimated from the voltammetries of [19]. This result is probably due to a different charge transfer rate through the adsorbed organic layer [27]. According to this approach, an increased thickness of the adsorbed layer would correspond to a decreased Tafel slope value. In the aqueous solutions, no substantial differences have been observed in β_c and i_L, in the presence or in the absence of TBAP.

Conclusions

Silver electrodeposition from water–acetonitrile mixed solvents has been investigated by means of SERS spectroscopy. Our experiments highlighted the hydrolysis reaction of acetonitrile giving rise to acetamide and then to acetic acid and NH_3. This reaction seems to be due to an electrocatalytic activity of the silver clusters growing onto the electrode surface during electrodeposition. The effects of the addition of the specifically adsorbing tetrabuthylammonium cation were also investigated. The ammonium quaternary compound is adsorbed onto the silver electrode already at low cathodic overpotentials and tilted on increasing the cathodic overpotential.

The values of cathodic Tafel slope and limiting current density, estimated from voltammetric data, are coherent with the kinetic theory for mixed solvents based on ion-transfer-controlled reduction rate and confirm the remarkable grain-refining activity of TBAP, observed in SEM micrographs of Ag layers deposited.

References

1. Galus Z (1995) In: Gerischer H, Tobias CW (eds) Advances in electrochemical science and engineering. VCH, Weinheim
2. Chen R, Xu D, Gao G, Gui L (2004) Electrochim Acta 49:2243 doi:10.1016/j.electacta.2004.01.004
3. Gu R, Cao P, Sun YH, Tian Z (2002) J Electroanal Chem 528:121 doi:10.1016/S0022-0728(02)00898-7
4. Cao P, Gu R, Qiu L, Sun R, Ren B, Tian Z (2003) Surf Sci 531:217 doi:10.1016/S0039-6028(03)00543-0
5. Doubova LM, Daolio S, Pagura C, De Battisti A, Transatti S (2003) Russ J Electrochem 39(2):164 doi:10.1023/A:1022308925322
6. Kuznetsov VV, Skibina LM, Loskutnikova IN (2000) Prot Metab 36(6):565 doi:10.1023/A:1026633312361
7. Kuznetsov VV, Skibina LM, Loskutnikova IN, Alekseev YE (2001) Prot. Metab 37(1):31 doi:10.1023/A:1004881400861
8. Peng X, Xiang C, Xie Q, Kang Q, Yao S (2006) J Electroanal Chem 591:74 doi:10.1016/j.jelechem.2006.03.025
9. Watanabe T (2004) Nano-Plating. Elsevier, Tokyo
10. Ardizzone S, Cappelletti G, Mussini PR, Rondinini S, Doubova LM (2003) Russ J Electrochem 39(2):170 doi:10.1023/A:1022361009393
11. Fleischmann M, Hendra PJ, Mcquillan AJ (1974) Chem Phys Lett 26:163 doi:10.1016/0009-2614(74)85388-1
12. Kaminskaia NV, Kostiæ NM (1966) J Chem Soc, Dalton Trans 3677
13. Venardou E, Garcia-Verdugo E, Barlow SJ, Gorbaty YE, Poliakoff M (2004) Vib Spectrosc 35:103 doi:10.1016/j.vibspec.2003.12.003
14. Lee GR, Crayston JA (1996) Polyhedron 15:1817 doi:10.1016/0277-5387(95)00432-7
15. Luo RS, Mao XA, Pan ZQ, Luo QH (2000) Spectrochim Acta A Mol Biomol Spectrosc 56:1675 doi:10.1016/S1386-1425(00)00235-3
16. Barbosa LAMM, van Santen RA (2000) J Mol Struct 497:173
17. Cariati E, Dragonetti C, Manassero L, Roberto D, Tessore F, Lucenti E (2003) J Mol Catal Chem 204:279 doi:10.1016/S1381-1169(03)00309-1
18. Mountain RD (2001) Int J Thermophys 22:101 doi:10.1023/A:1006707619435
19. Mele C, Bozzini B, Rondinini S, D'Urzo L, Romanello V, Tondo E, Minguzzi A, Vertova A (2008) Silver electrodeposition from water–acetonitrile mixed solvents and mixed electrolytes, in the presence of tetrabutylammonium perchlorate. Part I-Electrochemical nucleation on glassy carbon electrode. J Solid State Electrochem (in press) doi:10.1007/s10008-008-0732-y

20. Irish DE, Hill IR, Archambault P, Atkinson GF (1985) J Solution Chem 14:221 doi:10.1007/BF00647064
21. Mernagh TP, Cooney RP (1984) J Electroanal Chem 177:139 doi:10.1016/0022-0728(84)80218-1
22. Colthup NB, Daly LH, Wiberley SE (1990) Introduction to infrared and Raman spectroscopy. Academic, Boston
23. Kijima M, Toyabe T, Shirakawa H, Kawata S, Kyotani H, Nakamura Y, Endo T (1997) Synth Met 86:2279 doi:10.1016/S0379-6779(97)81125-3
24. Han G, Shi G, Yuan J, Chen F (2004) J Mater Sci 39:4451 doi:10.1023/B:JMSC.0000034137.82383.47
25. Redondo MI, Sánchez de la Blanca E, García MV, Raso MA, Tortajada J, González-Tejera MJ (2001) Synth Met 122:431 doi:10.1016/S0379-6779(00)00563-4
26. Hubin A, Gonnissen D, Simons W, Vereecken J (2007) J Electroanal Chem 600:142 doi:10.1016/j.jelechem.2006.05.017
27. Kahn SUM (1988) J Phys Chem 92:2541 doi:10.1021/j100320a029